

Turning up the spin, turning on single-molecule magnetism: from $S = 1$ to $S = 7$ in a $[\text{Mn}_8]$ cluster *via* ligand induced structural distortion†

Constantinos J. Milios,^a Ross Inglis,^a Alina Vinslava,^b Alessandro Prescimone,^a Simon Parsons,^a Spyros P. Perlepes,^c George Christou^b and Euan K. Brechin^{*a}

Received (in Cambridge, UK) 1st March 2007, Accepted 13th April 2007

First published as an Advance Article on the web 3rd May 2007

DOI: 10.1039/b703089d

The spin ground state of a $[\text{Mn}^{\text{III}}_6\text{Mn}^{\text{II}}_2]$ cluster has been deliberately switched from $S = 1$ to $S = 7$ upon designed ligand substitution.

Recent years have witnessed a vast increase in the number of coordination compounds, mainly transition metal clusters, that display interesting magnetic properties. This is perhaps not surprising given that it has been over a decade and a half since the first discovery of molecules that could behave as nanomagnets at very low temperatures. Such molecules, now termed Single-Molecule Magnets (SMMs), represent the ultimate downscale limit of magnetic devices that may potentially be used in applications such as quantum computation and information storage.^{1–4} Their intrinsic behaviour is due to the combination of a relatively large spin ground state and Ising-type anisotropy, which creates an energy barrier for the re-orientation of magnetisation. The prototype $[\text{Mn}_{12}\text{OAc}]$ SMM remains by far the most widely studied example of such a molecule, because, until recently,⁵ it remained the molecule with the largest energy barrier. One of our strategies for making new SMMs involves the use of derivatized salicylaldoximes (R-saoH₂) as key bridging ligands, and this has resulted in the formation of a family of hexametallc SMMs of general formula $[\text{Mn}^{\text{III}}_6\text{O}_2(\text{R-sao})_6(\text{O}_2\text{CR})_2(\text{R}'\text{OH})_{4-6}]$ (where R, R' = H, Me, Et, Ph, *etc.*). The first members of this family were the complexes $[\text{Mn}^{\text{III}}_6\text{O}_2(\text{sao})_6(\text{O}_2\text{CR})_2(\text{R}'\text{OH})_4]$ (saoH₂ = salicylaldoxime; R = H, Me, Ph, *etc.*), which are characterised by $S = 4$ ground states as a result of the ferromagnetic exchange between two antiferromagnetically coupled $[\text{Mn}^{\text{III}}_3]$ triangles.⁶ We speculated and later proved that the weak antiferromagnetic exchange mediated by the bridging oximate group (Mn–N–O–Mn) may be switched to a weak ferromagnetic exchange if the Mn–N–O–Mn moiety could be structurally distorted.⁷ This resulted in the formation of new members of the $[\text{Mn}^{\text{III}}_6\text{O}_2(\text{R-sao})_6(\text{O}_2\text{CR})_2(\text{R}'\text{OH})_{4-6}]$ family, which displayed dominant ferromagnetic exchange and $S = 12$ ground states.⁷ We are now investigating the general applicability of this approach, and herein report the syntheses, structures and magnetic properties of two analogous oximate-based octametallc Mn clusters with markedly different magnetic properties.

^aSchool of Chemistry, The University of Edinburgh, West Mains Road, Edinburgh, UK EH9 3JJ. E-mail: ebrechin@staffmail.ed.ac.uk; Tel: +44 (0)131-650-7545

^bChemistry Department, University of Florida, Gainesville, Florida, 32611-7200, USA

^cDepartment of Chemistry, University of Patras, 26504 Patras, Greece
† Electronic supplementary information (ESI) available: Crystallographic and experimental details. See DOI: 10.1039/b703089d

Reaction of the solution-stable $[\text{Mn}^{\text{III}}_6\text{O}_2(\text{naph-sao})_6(\text{O}_2\text{CPh})_2(\text{EtOH})_6]$ (**1**, naph-saoH₂ = 2-hydroxy-1-naphthaldoxime) with 1 equivalent of both $\text{Mn}(\text{ClO}_4)_2 \cdot 6\text{H}_2\text{O}$ and NaN_3 in MeOH leads to the formation of $[\text{Mn}^{\text{III}}_6\text{Mn}^{\text{II}}_2\text{O}_2(\text{naph-sao})_6(\text{N}_3)_6(\text{MeOH})_8] \cdot 10\text{MeOH}$ (**2**·10MeOH) after approximately 4 days of slow evaporation. Reaction of 1 equivalent of **2**·10MeOH with a large excess of Me-saoH₂ (2-hydroxyphenylethanone oxime) in $\text{CH}_2\text{Cl}_2/\text{MeOH}$ gave the complex $[\text{Mn}^{\text{III}}_6\text{Mn}^{\text{II}}_2\text{O}_2(\text{Me-sao})_6(\text{N}_3)_6(\text{MeOH})_8] \cdot 10\text{MeOH}$ (**3**·10 MeOH).‡

Complexes **2** and **3** have similar structures (Fig. 1 and Fig. 2), crystallizing in the triclinic space group $P-1$,§ which effectively result from the structure of **1** with two additional metal caps to the ‘upper’ and ‘lower’ triangular faces. The core consists of a bi-capped non-planar $[\text{Mn}^{\text{III}}_6(\mu_3\text{-O}^{2-})_2(\mu_3\text{-OR})_2]^{12+}$ unit of two offset, stacked $[\text{Mn}^{\text{III}}_3(\mu_3\text{-O}^{2-})]^{7+}$ triangular sub-units. Each sub-unit contains three fully deprotonated R-sao²⁻ ligands that bridge between the metal centres in the ‘equatorial’ plane of the three metals: two in a $\eta^1:\eta^1:\eta^1:\mu_2$ fashion and one in a $\eta^1:\eta^2:\eta^1:\mu_3$ fashion. The latter involves the ligand bridging to the second triangular sub-unit *via* an oximate oxygen. Each sub-unit is capped with one Mn^{II} ion *via* three *end-on* N_3^- ions (with $\text{Mn}^{\text{III}}\text{–N–Mn}^{\text{II}}$ angles ranging from 118 to 122°), resulting in an overall $[\text{Mn}^{\text{III}}_6\text{Mn}^{\text{II}}_2\text{O}_2(\text{NO})_6(\text{N}_3)_6]^{6+}$ core. The coordination of the Mn^{II} ion is completed by the presence of three MeOH molecules. Four of the six Mn^{III} ions (Mn2, Mn3 and s.e.) are six-coordinate and in distorted octahedral geometries, while the remaining two (Mn1 and s.e.) have square pyramidal geometries with an additional weak axial contact to a phenolato oxygen atom. The Jahn–Teller axes are approximately parallel, lying perpendicular to the $[\text{Mn}^{\text{III}}_3]$ planes. The two Mn^{II} centres (Mn4) are six-coordinate, adopting a

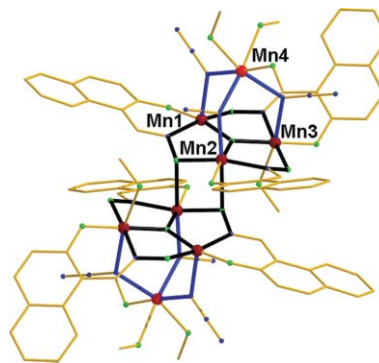


Fig. 1 The molecular structure of complex **2** highlighting the $[\text{Mn}^{\text{III}}_6\text{Mn}^{\text{II}}_2\text{O}_2(\text{NO})_6(\text{N}_3)_6]^{6+}$ core. Colour code: Mn^{II} = red, Mn^{III} = brown, O = green, N = blue and C = yellow.

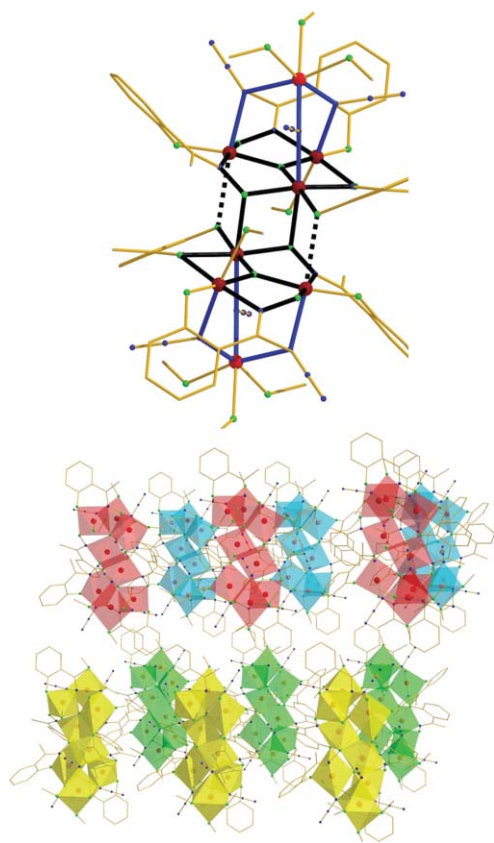


Fig. 2 Top: The molecular structure of complex **3** with its $[\text{Mn}^{\text{III}}_6\text{Mn}^{\text{II}}_2\text{O}_2(\text{NO})_6(\text{N}_3)_6]^{6+}$ core highlighted. Bottom: The packing of complex **3** in the crystal.

slightly distorted octahedral geometry. The inversion centre of each $[\text{Mn}_8]$ molecule lies on either a unit cell edge (**2**) or on a corner of the unit cell (**3**), with each cluster being oriented in the same direction (Fig. 2). The large number of alcohol solvate molecules associated with both **2** and **3** lie in the cavities between the metal clusters, and are involved in extensive hydrogen bonding interactions to each other, terminally-bound MeOH molecules and protruding N-atoms of the bridging azides. All of these interactions fall in the range $\sim 2.7\text{--}3.0$ Å. Complexes **2** and **3** join a handful of structurally and magnetically characterized Mn clusters at the $\text{Mn}^{\text{II}}_2\text{Mn}^{\text{III}}_6$ oxidation level.⁸

Although the two complexes (**2** and **3**) appear identical, there are two major differences: (a) the axial distance from the ‘square pyramidal’ Mn^{III} ion to the phenolato oxygen atom has decreased from 3.0 Å in **2** to 2.6 Å in **3**, and (b) the Mn–N–O–Mn torsion angles have increased significantly from 34.4° (Mn1–Mn3), 30.5° (Mn2–Mn3) and 28.8° (Mn1–Mn2) in **2** to 39.8° (Mn1–Mn3), 36.9° (Mn2–Mn3) and 40.0° (Mn1–Mn2) in **3**. Both effects may be attributed to the fact that the Me-sao²⁻ ligand has induced a structural distortion on the cluster in the shape of a twisting of the Mn–N–O–Mn moiety, due to the presence of the pendant or ‘non-planar’ $-\text{CH}_3$ group on the oximate carbon. We have previously speculated that a ‘switch’ in the exchange interaction from antiferromagnetic to ferromagnetic in the $[\text{Mn}_6]$ family of oximate clusters occurs at a Mn–O–N–Mn torsion angle of approximately 30–31°. This would suggest that the six central Mn^{III} ions in **3** should be ferromagnetically coupled.

The initial idea of employing azide in a reaction with complex **1** and a source of Mn^{II} was to attach Mn^{II} ions to the upper and lower faces of the cluster in the hope that we would generate an octametallate $[\text{Mn}^{\text{III}}_6\text{Mn}^{\text{II}}_2]$ cluster, in which the *end-on* azides would promote ferromagnetic exchange between the original $[\text{Mn}_6]$ (**1**, $S = 4$) core and the two attached Mn^{II} ($S = 5/2$) ions, making a molecule with a spin ground state of $S = 9$. However, despite the successful synthetic strategy, dc susceptibility measurements of **2** (Fig. 3) showed that this interaction is, in fact, antiferromagnetic. Measurements performed on a microcrystalline sample in the temperature range 300–5 K in an applied field of 0.1 T showed a continual decrease from a value of 25.80 $\text{cm}^3 \text{mol}^{-1} \text{K}$ at 300 K (very close to the spin-only ($g = 2$) value of 26.75 $\text{cm}^3 \text{mol}^{-1} \text{K}$ expected for six high-spin Mn^{III} and two high-spin Mn^{II} ions) to a value of 2.12 $\text{cm}^3 \text{mol}^{-1} \text{K}$ at 5 K, suggesting a $S \approx 1$ ground state. This initially disappointing result was tempered by our ability to ‘twist’ the oximate linkage by simply substituting naph-sao²⁻ with Me-sao²⁻.

Indeed, complex **3** displays completely different magnetic behaviour, as shown in Fig. 3. The $\chi_{\text{M}}T$ value of 25.83 $\text{cm}^3 \text{mol}^{-1} \text{K}$ at 300 K remains almost constant until ~ 100 K, below which it decreases rapidly to a minimum value of 20.94 $\text{cm}^3 \text{mol}^{-1} \text{K}$ at 17 K, before rising to a maximum of 22.65 $\text{cm}^3 \text{mol}^{-1} \text{K}$ at 8 K. Below 8 K, it decreases again to a value of 20.8 $\text{cm}^3 \text{mol}^{-1} \text{K}$ at 5 K. This behaviour is consistent with the presence of competing ferromagnetic and antiferromagnetic interactions, with the low temperature maximum suggesting a $S \approx 7$ ground state. The low temperature decrease below 8 K can be assigned to intermolecular interactions and/or effects of zero-field splitting. Given the striking differences in the magnetic behaviour of two ‘isostructural’ complexes, we attempted to simulate the data for one of them as a means to further elucidate the observed behaviour. We were able to satisfactorily simulate the data for **3** by assuming the 2- J model shown in Fig. 3, which describes a ferromagnetic $[\text{Mn}^{\text{III}}_6]$ moiety antiferromagnetically coupled to the capping Mn^{II} ions. Employing the spin Hamiltonian (\hat{H}) in eqn. (1)

$$\hat{H} = -2J_1(\hat{S}_1\hat{S}_2 + \hat{S}_2\hat{S}_3 + \hat{S}_1\hat{S}_3 + \hat{S}_4\hat{S}_5 + \hat{S}_4\hat{S}_6 + \hat{S}_5\hat{S}_6 + \hat{S}_1\hat{S}_4 + \hat{S}_1\hat{S}_6 + \hat{S}_3\hat{S}_6) - 2J_2(\hat{S}_1\hat{S}_7 + \hat{S}_2\hat{S}_7 + \hat{S}_7\hat{S}_3 + \hat{S}_4\hat{S}_8 + \hat{S}_5\hat{S}_8 + \hat{S}_6\hat{S}_8) \quad (1)$$

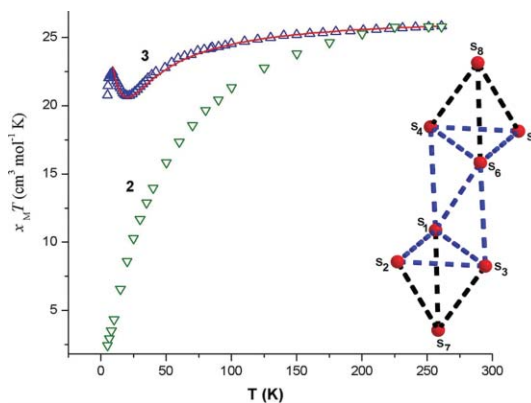


Fig. 3 Plot of $\chi_{\text{M}}T$ vs. T for complexes **2** and **3**. The solid line represents a simulation of the data in the temperature range 275–5 K (see text for details). Inset: The exchange interaction models used for **3**. Blue-dotted line: J_1 , black-dotted line: J_2 . The view is the same as in Fig. 2.

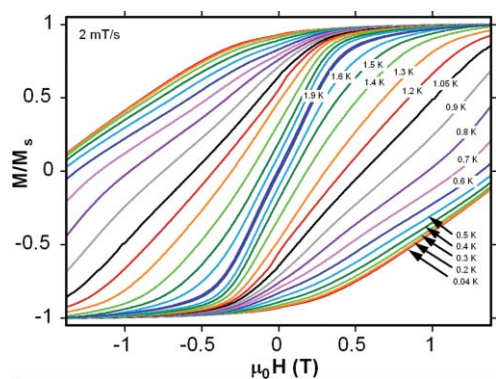


Fig. 4 Magnetisation vs. field hysteresis loops for a single crystal of **3** at the indicated temperatures and at a field sweep rate of 2 mT s⁻¹. M is normalised to its saturation value.

afforded the parameters $J_1 = +0.6$ cm⁻¹, $J_2 = -1.4$ cm⁻¹ and $g = 2.00$, which gives a ground state of $S = 7$, with the first ($S = 6$) and second ($S = 5$) excited states 4 and 9 cm⁻¹ higher in energy, respectively. This simulation allows us to infer a description of two Mn^{II} ions antiferromagnetically coupled to a $S = 12$ [Mn^{III}₆] sub-core in **3** and a possible description of the two Mn^{II} ions being antiferromagnetically coupled to a $S = 4$ [Mn^{III}₆] core in **2**.

Magnetization (M) data were collected for **3** in the magnetic field and temperature range 0.1–7 T and 1.8–7.0 K, respectively, but we could not obtain a good fit for the data by assuming that only the ground state was populated. Indeed, the magnetisation value rises continually with applied field. This suggests that the population of low lying excited states, even at these temperatures, is in agreement with the simulation of the dc susceptibility and the existence of a rather weak exchange between the metal centres. This was further confirmed by ac susceptibility measurements performed with a 3.5 G ac field oscillating at frequencies of up to 1500 Hz (Fig. S11†). The sloping $\chi_M' T$ vs. T plot over a relatively narrow temperature range was characteristic of low-lying excited states with S greater than that of the ground state, and which are increasingly populated as the temperature increases. Extrapolating the in-phase curve to 0 K from temperatures above approximately 6 K gives a $\chi_M' T$ value of ~ 19 cm³ mol⁻¹ K, which is suggestive of $S = 6 \pm 1$; the inset of Fig. S11† shows the $\chi_M' T$ vs. T plot for complex **2**, confirming $S = 1 \pm 1$. It is also interesting to note that both the in-phase (χ_M') and out-of-phase (χ_M'') signals for complex **3** show a small frequency dependence below approximately 5 K. Normally, these are taken as indicators of single-molecule magnetism behaviour. For well studied and well understood SMMs (Mn₁₂OAc, for example), the ratio of the magnitude of the in-phase to out-of-phase signal is usually in the range 2 : 1–10 : 1, but here it is ca. 60 : 1 and thus, in itself, is inconclusive evidence. We and others have previously commented that the only watertight proof for SMM behaviour is the presence of temperature and sweep rate dependent hysteresis loops in magnetization vs. field studies. Single crystal measurements of **3** performed on a micro-SQUID apparatus at temperatures down to 40 mK are shown in Fig. 4 and do indeed display such loops. They do not show the sharp step-like features indicative of quantum tunneling of the

magnetisation, but are instead smooth and “double-S-like” in shape, a situation typically seen for SMMs displaying weak intermolecular antiferromagnetic interactions, consistent with the crystal structure of **3**.

In conclusion, we have shown that the family of hexametallate clusters of general formula [Mn^{III}₆O₂(R-sao)₆(O₂CR)₂(R'OH)₄₋₆] are, despite having interesting magnetic properties in their own right, excellent building blocks for the synthesis of new clusters. Here, we demonstrated that a Mn₆ molecule can be capped by the simple addition of Mn^{II} and azide ions to make a closely related [Mn^{III}₆Mn^{II}₂] cluster. We also demonstrated that the spin ground state ($S \approx 1$) of the resultant cluster can be changed by inducing structural disorder at the oximate linkage; substitution of the ‘planar’ naphth-sao²⁻ ligand for the ‘non-planar’ Me-sao²⁻ ligand increased the Mn–N–O–Mn torsion angles significantly, and the result was a change in the magnitude and sign of the exchange interactions between the metals and a molecule displaying a much larger spin ground state ($S \approx 7$) and SMM behaviour. This suggests the deliberate ‘twisting’ of oximate groups as a general strategy for making high spin molecules and for turning low spin or diamagnetic ground state oximate-based clusters into SMMs. The concept of deliberate structural distortion may also be valid for a plethora of other polymetallic systems.

Notes and references

† Full details of the experimental microanalyses are given in the ESI.†
 § *Crystal data for complex 2*: C₈₄H₁₁₄Mn₈N₂₄O₃₂, $M = 2411.5$, dark brown block, triclinic, $P\bar{1}$, $a = 13.8273(3)$, $b = 15.3275(3)$, $c = 15.5166(4)$ Å, $\alpha = 111.6580(10)$, $\beta = 109.8920(10)$, $\gamma = 102.6120(10)^\circ$, $V = 2642.14(10)$ Å³, 61412 reflections collected of which 14863 were independent ($R_{\text{int}} = 0.0506$), 694 parameters and 12 restraints, $R1 = 0.0492$ [based on $F > 4\sigma(F)$], $wR2 = 0.1174$ (based on $F2$ and all data). CCDC 638207.

Crystal data for complex 3: C₆₆H₁₁₄Mn₈N₂₄O₃₂, $M = 2195.3$, black blocks, triclinic, $P\bar{1}$, $a = 11.698(2)$, $b = 12.608(3)$, $c = 17.019(3)$ Å, $\alpha = 76.05(3)$, $\beta = 82.03(3)$, $\gamma = 75.41(3)^\circ$, $V = 2349.4(9)$ Å³, 67762 reflections collected of which 9606 were independent ($R_{\text{int}} = 0.103$), 496 parameters and 18 restraints, $R1 = 0.0698$ [based on $F > 4\sigma(F)$], $wR2 = 0.0574$ (based on F using the $I > 2\sigma(I)$ data). CCDC 638208.

For crystallographic data in CIF or other electronic format see DOI: 10.1039/b703089d

- G. Christou, D. Gatteschi, D. N. Hendrickson and R. Sessoli, *MRS Bull.*, 2000, **25**, 66.
- D. Gatteschi and R. Sessoli, *Angew. Chem., Int. Ed.*, 2003, **42**, 268.
- R. Bircher, G. Chabousant, C. Dobe, H. U. Güdel, S. T. Ochsenein, A. Sieber and O. Waldmann, *Adv. Funct. Mater.*, 2006, **16**, 209.
- J. Tejada, E. M. Chudnovsky, E. del Barco, J. M. Hernandez and T. P. Spiller, *Nanotechnology*, 2001, **12**, 181.
- C. J. Milios, A. Vinslava, W. Wernsdorfer, S. Moggach, S. Parsons, S. P. Perlepes, G. Christou and E. K. Brechin, *J. Am. Chem. Soc.*, 2007, **129**, 2754.
- (a) C. J. Milios, C. P. Raptopoulou, A. Terzis, F. Lloret, R. Vicente, S. P. Perlepes and A. Escuer, *Angew. Chem., Int. Ed.*, 2003, **43**, 210; (b) C. J. Milios, A. Vinslava, A. Whittaker, S. Parsons, W. Wernsdorfer, G. Christou, S. P. Perlepes and E. K. Brechin, *Inorg. Chem.*, 2006, **45**, 5272.
- C. J. Milios, A. Vinslava, W. Wernsdorfer, P. A. Wood, S. Parsons, S. P. Perlepes, G. Christou and E. K. Brechin, *J. Am. Chem. Soc.*, 2007, **129**, 8.
- (a) M. W. Wemple, H.-L. Tsai, S. Wang, J. P. Claude, W. E. Streib, J. C. Huffman, D. N. Hendrickson and G. Christou, *Inorg. Chem.*, 1996, **35**, 6437; (b) E. K. Brechin, G. Christou, M. Soler, M. Helliwell and S. J. Teat, *Dalton Trans.*, 2003, 513.